HEAT AND MASS TRANSFER ON THE SURFACE OF A BODY WITH ROTATING NOSE SECTION AT HYPERSONIC FLOW VELOCITIES

N. A. Krasilov, V. A. Levin and S. A. Yunitskii

UDC 533.6.011.55

The influence of a body of revolution or just its nose section on the heat flux is investigated under strong gas injection for a variable flow rate around the contour.

A large number of papers [1-11] is devoted to the study of the aerodynamic characteristics of bodies from whose surface gas is injected. Injection with a constant gas flow rate around the body contour is examined in [1-5]. The case of variable injection (depending on the solution of the problem) is also studied in [6]. Gas injection concentrated in the neighborhood of the critical point is described in [7-10]. Flow around rotating bodies has been investigated earlier on the basis of parabolized Navier-Stokes equations [11] and the boundary layer [12]. Viscous gas flow around an axisymmetric blunt body rotating as a single whole has been studied in [13] in a broad range of Reynolds numbers from moderately low to high for constant and variable injection along the contour. An asymptotic solution of the problem has been obtained in the neighborhood of the stagnation point, as has also a numerical solution of the problem of the flow around a rotating sphere and paraboloid. It is shown that rotation in the whole considered range of Reynolds numbers and injected gas flow rate will result in an increase in the heat flux to the body, whose dependence on the longitudinal coordinate is not monotonic; the maximum is not reached at the stagnation point but at a point on the side surface of the body.

1. We consider stationary hypersonic laminar viscous compressible gas flow around a blunt axisymmetric body. We assume that either the whole body as a single whole, or its nose section, rotates. At high free-stream Mach numbers M_∞, moderate and high Reynolds numbers, the gas flow around a rotating axisymmetric body is described by the equations of the hypersonic viscous shock layer which have the following form in dimensionless variables

$$\begin{gathered}
\frac{\partial}{\partial x}(\rho r_w u)+\frac{\partial}{\partial y}(\rho r_w v)=0,\\
\rho\left(u\frac{\partial u}{\partial x}+v\frac{\partial u}{\partial y}-\frac{\sin\alpha}{r_w}w^2\right)=-\varepsilon\frac{\partial P}{\partial x}+\frac{\partial}{\partial y}\left(\frac{\mu}{K}\frac{\partial u}{\partial y}\right),\\
\rho\left(u\frac{\partial w}{\partial x}+v\frac{\partial w}{\partial y}+\frac{\sin\alpha}{r_w}uw\right)=\frac{\partial}{\partial y}\left(\frac{\mu}{K}\frac{\partial w}{\partial y}\right),\\
\rho\left(\varkappa u^2+\frac{\cos\alpha}{r_w}w^2\right)=\frac{\partial P}{\partial y},\\
\rho\left(u\frac{\partial T}{\partial x}+v\frac{\partial T}{\partial y}\right)=2\varepsilon u\frac{\partial P}{\partial x}+\frac{2\mu}{K}\left[\left(\frac{\partial u}{\partial y}\right)^2+\left(\frac{\partial w}{\partial y}\right)^2\right]+\frac{\partial}{\partial y}\left(\frac{\mu}{\sigma K}\frac{\partial T}{\partial y}\right),\quad P=\rho T,\ \mu=T^{\omega}.
\end{gathered}\tag{1}$$

These equations are written in an orthogonal curvilinear coordinate system (x, y, ϑ) coupled to the body surface. The relation between the dimensional and dimensionless variables is the following: the quantities x, $\varkappa$, r_w, z are referred to the body bluntness radius R, y to εR; the velocity vector components u, v, w to U_∞, εU_∞, U_∞; the density ρ to $\varepsilon^{-1}\rho_\infty$; the pressure P, temperature T, and enthalpy H to $\rho_\infty U_\infty^2$, T_0, $c_p T_0$.

On the shockwave we give modified Rankine—Hugoniot relations in the thin layer approximation

$$y=y_s(x):\ \rho\left(v-u\frac{\partial y_s}{\partial x}\right)=v_\infty,\ P=v_\infty^2,$$

Translated from Inzhenerno-Fizicheskii Zhurnal, Vol. 51, No. 6, pp. 940-946, December, 1986. Original article submitted September 23, 1985.

 0022-0841/86/5106-1412$12.50

$$v_\infty(u-u_\infty)=\frac{\mu}{K}\frac{\partial u}{\partial y},\quad v_\infty w=\frac{\mu}{K}\frac{\partial w}{\partial y},$$
$$v_\infty(H-H_\infty-v^2_\infty)=\frac{\mu}{\sigma K}\frac{\partial T}{\partial y}+\frac{2\mu}{K}\left(u\frac{\partial u}{\partial y}+w\frac{\partial w}{\partial y}\right). \tag{2}$$

On the body surface we consider values of the longitudinal and azimuthal velocity components and the injected gas flow rate and temperature known:

$$y=0:\ u=0,\ \rho v=G(x),\ T=T_w(x),$$
$$w=\begin{cases} Br_w(x), & 0\leqslant x\leqslant x_B,\\ 0, & x_B<x\leqslant x_M.\end{cases} \tag{3}$$

For a numerical solution the system (1)-(3) is written in Dorodnitsyn type variables. Calculations were performed using an implicit finite-difference scheme [14]. Details are expounded in [13]. In all the computations it was assumed that $\omega = 0.5$; $\sigma = 0.71$; $T_w = 0.1$; $\varepsilon = 0.1$.

2. FLOW AROUND A ROTATING BODY

In connection with the application of gas injection to reduce the heat flux, there is the problem of determining the best method of organizing the injection. Thus, for instance, gas can be injected through an orifice in the nose or more uniformly over the contour, through the porous surface. To model different gas injection methods, the heat and mass transfer on the surface of a rotating sphere was investigated for $X_B = X_M$. We give the flow rate of the gas being injected in the form

$$G=G_0\exp[-(t/t_0)^2]. \tag{4}$$

The parameter t depends on the longitudinal coordinate x or the distance measured along the Oz axis. Let us set $t \equiv x$ and $t_0 \equiv x_0$. Since the magnitude of the total injected gas flow rate

$$G_\Sigma=2\pi\int_0^{x_M} G(x)r_w(x)\,dx$$

is always limited in practice, the optimal injection distribution law (4) that assures a reduction in the maximum value of the heat flux to the body is sought expediently for a fixed value of G_Σ. During the calculations, after x_0 has been given, the condition G_Σ = const is assured by selecting the quantity G_0 defined by the formula

$$G_0=G_\Sigma\Big/\left\{2\pi\int_0^{x_M}\exp[-(x/x_0)^2]r_w(x)\,dx\right\}.$$

Let us examine the results of computing the flow around a rotating sphere for different values of x_0. As is seen from Fig. 1, as x_0 diminishes the injection at the stagnation point becomes all the more significant, and for $x_0 = 0.2$, $B = 0$ an entire circle $0 \le x \le 0.15$ appears in which the thermal flux is practically zero. As x_0 increases, the thermal flux at the stagnation point grows and later diminishes somewhat around the contour. For $x_0 = 1.2$ and $x_0 = 0.2$ the maximal value of the heat flux is greater than for $x_0 = 0.4$. Therefore, the dependence of the maximal value of the thermal flux q_{max} on the quantity x_0 is not monotonic.

A number of additional computations in the range of values [0.2, 1.2] for x_0 was performed to obtain the function $q_{max}(x_0)$. Analysis of the results obtained showed that for all the values of the rotation parameter B this dependence has a minimum (see Fig. 2). For the values $0 \le B \le 1$ the quantity q_{max} reaches the minimum for $0.4 \le x_0 \le 0.6$. This means that an optimal injection distribution law (4) exists with a fixed total flow rate for which the value of q_{max} is minimal. Gas injection according to the law (4) for $x_0 \in [0.4, 0.6]$ is more efficient than injection with a uniform flow rate distribution for the same value of G_Σ. Thus the growth of x_0 to the value 1, to which an almost uniform flow rate distribution of the injected gas over the sphere surface corresponds, will result in an increase in the maximal thermal flux by 15-50% as compared with the optimal value (the greatest value corresponds to B = 0 and the least to B = 1). Body rotation results in the growth of q_{max} and an increase in the optimal value of x_0.

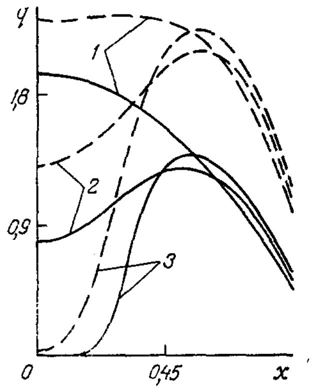

Fig. 1

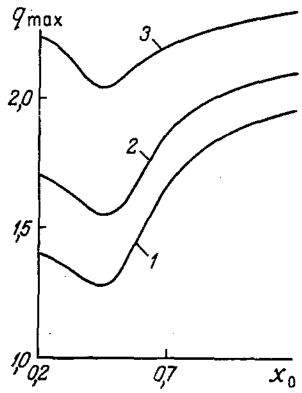

Fig. 2

Fig. 1. Distribution of the dimensionless thermal flux q on a sphere for G_ε = 0.063; Re = 500; B = 0 (solid curves) and 1 (dashes); 1) x_0 = 1.2; 2) 0.4; 3) 0.2.

Fig. 2. The dependence of values of the maximal thermal flux q_{max} on a sphere on x_0 for G_Σ = 0.063; Re = 500 and different values of B: 1) B = 0; 2) 0.6; 3) 1.0.

The optimal injection distribution according to the law (4) was also investigated for Re = $5 \cdot 10^3$. The greatest reduction in the thermal flux maximum is here assured, as for Re = 500 also, by the value of $x_0 \in [0.4, 0.6]$. The selection of x_0 outside the interval mentioned results in an increase in q_{max}, where in the case of the flow around a nonrotating sphere the value of q_{max} grows more abruptly in the domain $x_0 \geq 0.6$ than in the domain $x_0 \leq 0.4$.

3. GAS INJECTION ON THE ROTATING NOSE SECTION

In this case the boundary value for the aximuthal velocity component undergoes a discontinuity at the point x_B. It follows from an analysis of the Navier-Stokes equations that the terms with second derivatives with respect to x can be neglected in the whole flow domain outside a small neighborhood of the point of discontinuity. The magnitude of this neighborhood is of the order of the boundary layer thickness.

Solutions of parabolic equations with discontinuous boundary conditions were studied earlier in a number of papers [4, 10, 15-18]. Thus, a solution is constructed in [15] by using the joining of two expansions, external (flow up to the discontinuity) and internal (flow after the discontinuity). The flow in the boundary layer was examined in the presence of a discontinuity in the body surface curvature [16], a discontinuous flow rate for the gas being injected [7, 10, 18], a jump change in the longitudinal body surface velocity [17], and a discontinuous value of the wall temperature [18]. In [7, 17, 18], computations were compared with experimental data and it was shown that the perturbation propagation domain upstream from the point of discontinuity is not large, while a computation within the framework of equations of parabolic type (boundary layer equations) is in satisfactory agreement with experiment. The necessity to select a more shallow step in the longitudinal direction for a difference mesh outside the point of discontinuity of the boundary conditions is indicated in [16].

The possibility of applying a numerical algorithm was investigated before performing the serial computations, and the optimal difference mesh spacing in the neighborhood of the point of discontinuity was determined. To find the solution for $x \leq x_B$ a uniform difference mesh in the longitudinal coordinate was used with a discretization step of $\Delta x = 0.0475$, while for $x > x_B$ a nonuniform mesh was used whose nodes shrunk in the neighborhood of the point x_B. The minimal value of the step Δx_{min} was selected equal to $4 \cdot 10^{-4}$. The mesh contained 41 nodes along the normal to the body surface.

Let us consider the flow around a paraboloid with a rotating nose section where gas is injected from the nose section at a variable flow rate (4) around the contour for $t \equiv z$, $t_0 \equiv z_0 = 0.14$. The nose section of the body makes the free stream overspeed; consequently, the maximum of the azimuthal velocity vector component w is reached on the body surface. For $x > x_B$ we have w = 0 on the body surface; however, within the shock layer the gas particles have

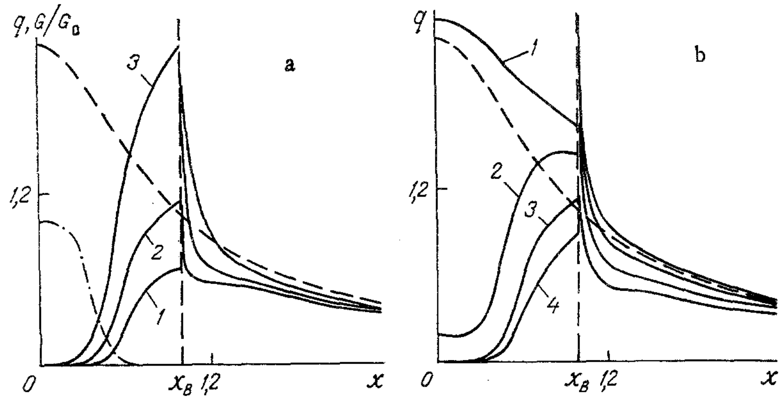

Fig. 3. Dependence of the dimensionless thermal flux on the surface of a paraboloid with rotating nose section on x for Re = $5 \cdot 10^3$ (dashed curve, G = 0, B = 0): a) solid curves, G_0 = 0.2, z_0 = 0.14, x_B = 1.0, B = 0.3 (1), 0.6 (2), 1.0 (3); dash-dot, the quantity G/G_0; b) solid curves, B = 0.6, z_0 = 0.14, x_B = 1.0, G_0 = 0 (1), 0.1 (2), 0.2 (3), 0.3 (4).

TABLE 1. Values of the Dimensionless Total Thermal Flux Coefficient $c_q \cdot 10^2$ on a Paraboloid with a Rotating Nose Section for Re = $5 \cdot 10^3$

G_0	B	$c_q \cdot 10^2$			
		$z=z_B=0,4$	$z=0,84$	$z=1,51$	$z=2,40$
0,0	0,0	2,48	2,08	1,73	1,46
0,2	0,3	0,68	0,90	0,96	0,93
0,2	0,6	1,12	1,29	1,21	1,10
0,1	0,6	1,80	1,77	1,53	1,33
0,3	0,6	0,80	0,95	0,95	0,91

a nonzero azimuthal velocity vector component because of the convective transfer of momentum in the longitudinal direction. Therefore, w achieves the maximum within the shock layer on the tail section of the body. The quantity w_{max} decreases with removal downstream from the point x_B. The friction coefficient τ_2 undergoes a discontinuity at the point $x = x_B$ and it is negative for $x > x_B$ since the gas, oversped by the nose section of the body, interacts with the fixed tail section. The quantity is $\tau_2 \simeq 0$ for $x \gtrsim 2.5$.

Now let us examine the influence of rotation of the nose section for different values of the rotation parameter and fixed gas injection on the heat flux to the body, and let us make a comparison with the case of a nonrotating and impenetrable body. The results of computations are presented in Fig. 3. For B = 1.0, G_0 = 0.2 the gas injection in the neighborhood of the body stagnation point results in a substantial reduction in the thermal flux only for $x \le 0.5$. Furthermore, the flow rate of the gas being injected around the body contour decreases while the kinetic energy dissipation associated with the rotation grows. Heating of the gas in the shock layer occurs and the thermal flux to the body increases sharply. For $x = x_B$ the maximal value of the thermal flux is achieved on rotating nose section, being only a somewhat smaller value at the stagnation point for G = 0, B = 0. For B = 1.0, G_0 = 0.2 the thermal flux on a considerable portion of the rotating nose section surface exceeds the thermal flux to a nonrotating impenetrable body. As the rotation parameter diminishes to the value B = 0.6 (curve 2, Fig. 3a), the thermal flux on the rotating nose is less than in the case of no injection and rotation, with the exception of a small region near the point x_B. For B = 0.3 injection with a flow rate G_0 = 0.2 results is a still greater reduction in the heat flux: in this case, on the nose section q_{max} is ~30% of the value for B = 0, G = 0. Exactly as for B = 1, for B = 0.6 and 0.3 the maximum heat flux on the body with rotating nose section is reached in the neighborhood of the point $x = x_B$.

Rotation of the body nose section exerts influence on the flow around the nonrotating tail section. For instance, let us consider the value of the thermal flux at the point x = 1.4, located on the nonrotating section of the body near the point of discontinuity in the boundary conditions. For B = 1.0, G_0 = 0.2, injection results in an insignificant diminution in the heat flux (less than 10%). For B = 0.6 this diminution is 23%, and for B = 0.3 around 30%. At the point x = 2.8 located considerably below the point of boundary condition discontinuity, the difference between the values of the thermal flux for all the cases considered is not large and is 11%.

The influence of injection and rotation on the total thermal flux coefficient to the body $c_q = Q/0.5\rho_\infty U_\infty^3 S_M$ is illustrated in the table for different values of z. For B = 1.0, G_0 = 0.2 the total thermal flux for the mentioned values of z is practically the same as for B = 0, G = 0. Therefore, for a fixed value of the injected gas flow rate G_0 = 0.2, the maximally achievable value of the rotation parameter that will assure a reduction in the local and total thermal flux to the body is B = 0.6.

The problem of determining the injected gas flow rate that would assure the necessary reduction in the maximal flux can be formulated analogously for a given minimal value of the rotation parameter B. As is seen from Fig. 3b, a diminution in the injected gas flow rate for B = 0.6 results in the growth of the local and total thermal flux (see the table also). It follows from the results presented above that in this case the minimal value of the injection parameter that would assure a reduction in the thermal flux to the body is 0.2.

The relative influence of rotation on the thermal flux depends in a substantial manner on the streamlining conditions. Thus, for instance, for Re = $5 \cdot 10^3$ the thermal flux in the neighborhood of the stagnation point of an impenetrable rotating body for B = 0.3 exceeds the corresponding value for B = 0 by 1.7%. For gas injection from the body surface the magnitude of the thermal flux decreases and the influence of rotation becomes more noticeable: for G = 0.02 and 0.06 the increase in the thermal flux because of rotation is 4.4 and 37.5%; respectively. In regimes close to strong injection, the thermal flux to the surface of a rotating body is several times greater than to a nonrotating body: it grows 2.1-4.3 times for G = 0.08-0.1.

NOTATION

x, distance along the body generatrix; y, distance along the normal to the body surface; ϑ, meridian angle; Oz, body axis of symmetry; z, distance along Oz measured from the nose; α, angle between the tangent to a body surface element and Oz; κ, longitudinal surface curvature; r_w, distance to the Oz axis; R, bluntness radius; U, u, v, w, velocity vector modulus and its components; $H = T + u^2 + w^2$, total enthalpy; c_p, c_V, specific heats for constant pressure and volume; $\gamma = c_p/c_V$, adiabatic index; λ, μ, heat conductivity and viscosity coefficients; Ω, angular velocity of the body; $Re = \rho_\infty U_\infty R/\mu_0$, $\sigma = \mu c_p/\lambda$, M_∞, Reynolds, Prandtl, and Mach numbers; $T_0 = U_\infty^2/2c_p$, stagnation temperature; $\mu_0 = \mu(T_0)$, viscosity at the temperature T_0; $B = \Omega R/U_\infty$, rotation parameter; $G = \rho w^V w/\rho_\infty U_\infty$, dimensionless injected gas flow rate; $\varepsilon = (\gamma - 1)/2\gamma$, $K = \varepsilon \cdot Re$, dimensionless parameters; S_M, dimensional area of the middle section; $q = \sqrt{Re}\frac{\mu}{\sigma K}\left.\frac{\partial T}{\partial y}\right|_w$, dimensionless thermal flux; $\tau_2 = -\frac{\sqrt{Re}}{\cos\alpha}\frac{2\mu}{K}\left.\frac{\partial w}{\partial y}\right|_w$, dimensionless friction coefficient; Q, total thermal flux to the body side surface from the stagnation point to the section $z = z_M$. Subscripts: ∞, at infinity; s, on the compression shock; w, on the body surface; B, at the point connecting the nose and tail sections of the body; M, at the section of the middle of the body; min and max, minimal and maximal value.

LITERATURE CITED

1. G. A. Tirskii, Nauchn. Trudy No. 39 [in Russian], M. V. Lomonosov Moscow State Univ., Institute of Mechanics (1975), pp. 5-38.
2. S. A. Vasilevskii and G. A. Tirskii, Aerodynamics of Hypersonic Flows in the Presence of Injection [in Russian], Moscow (1979), pp. 87-98.
3. S. A. Yunitskii, "Numerical investigation of the hypersonic spatial viscous shock layer on a permeable surface," Candidate's Dissertation, Moscow (1981).
4. É. A. Gershbein and S. V. Peigin, Izv. Akad. Nauk SSSR, Mekh. Zhidk. Gaza, No. 5, 28-36 (1979).
5. V. I. Zinchenko and E. N. Putyatina, Inzh.-Fiz. Zh., 45, No. 1, 11-21 (1983).
6. I. I. Vigdorovich and V. A. Levin, Supersonic Flow around Bodies with Intense Injection [in Russian], Moscow (1983).
7. É. A. Stepanov, Aerodynamic Heating at Supersonic Flow Velocities [in Russian], Trudy TsAGI, No. 1692 (1975), pp. 67-129.
8. V. A. Antonov and A. M. Grishin, Zh. Prikl. Mekh. Tekh. Fiz., No. 4, 86-92 (1982).

9. Yu. N. Ermak, Zh. Prikl. Mekh. Tekh. Fiz., No. 6, 94-101 (1983).
10. A. M. Antonov, V. A. Zakrevskii, and A. P. Komashenko, Mathematical Methods of Heat and Mass Transfer [in Russian], Moscow (1984), pp. 165-168.
11. M. D. Kim and C. H. Lewis, Aerospace Eng., 1, No. 12, 90-98 (1983).
12. A. N. Pokrovskii, V. N. Shmanenkov, and V. M. Shchuchinov, Izv. Akad. Nauk SSSR, Mekh. Zhidk. Gaza, No. 3, 34-39 (1984).
13. N. A. Krasilov, V. A. Levin, and S. A. Yunitskii, Izv. Akad. Nauk SSSR, Mekh. Zhidk. Gaza, No. 1, 106-114 (1986).
14. I. V. Petukhov, Numerical Methods of Solving Differential and Integral Equations and Quadrature Methods [in Russian], Moscow (1964), pp. 304-325.
15. V. I. Eliseev, Inzh.-Fiz. Zh., 24, No. 3, 445-452 (1973).
16. A. L. Ankudinov, Zh. Vychisl. Mat. Mat. Fiz., 5, No. 5, 960-966 (1965).
17. J. S. Tennant and T. Yang, AIAA J., 11, No. 8, 1156-1160 (1973).
18. V. A. Aleksin and V. D. Sovershennyi, Turbulent Flows [in Russian], Moscow (1977), pp. 55-63.

BREAKAWAY FLOW AROUND GRIDS OF NONCIRCULAR TUBES

M. I. Nisht and A. G. Sudakov

UDC 532.5.013.12:532.54

On the basis of the discrete-vortex method, breakaway flow around a single-row assembly (grid) of tubes of square, rectangular, and triangular cross section is investigated.

1. Loss of pressure (resistance) and heat transfer in the transverse flow around tube assemblies are determined primarily by the character of the fluid flow close to the tube surfaces, which, in turn, depends on the geometric parameters of the assembly (the shape of the tube cross section, their distance apart, etc.) and on the conditions of flow around the assembly (Reynolds number Re). In the range of Reynolds numbers characteristic in practice, flow around the tubes is always of breakaway type and is accompanied by the formation of a developed accompanying wake behind the tubes [1].

The difficulty in solving the complete Navier–Stokes or Reynolds equations for describing breakaway flow conditions at bodies with limitingly high Re, when the influence of molecular viscosity on the flow is slight, has led to the development of calculation methods based on the model of an ideal medium. An example of the realization of this approach is the currently widespread discrete-vortex method [2]. The agreement between the calculation results obtained by this method and experimental data provides the basis for the assumption that this approach is justified in considering completely developed turbulent flow, when the flow-breakaway point at the surface of the body is known in advance.

In the present work, results obtained by the discrete-vortex method are given for the resistance of a single-row assembly (grid) of tubes of square, rectangular, and triangular cross section. Grids consisting of plates are also considered. It is supposed that flow breakaway at these bodies occurs for tubes at points of discontinuity of the cross section and for plates at their sharp edges. Note that the calculation results for the flow obtained by the discrete-vortex method are the initial data for calculating the boundary layer at tube surfaces and the heat transfer between the tubes and the flow.

2. The basic assumptions of the discrete-vortex method for calculating various breakaway flows were outlined in [2]; they reduce to the following. The medium is ideal and incompressible. Breakaway is modeled using vortex surfaces that are convergent in the flow. The character of the limiting flow in the general case is established by studying the whole process of flow formation over time.

Translated from Inzhenerno-Fizicheskii Zhurnal, Vol. 51, No. 6, pp. 947-951, December, 1986. Original article submitted November 19, 1985.

